8-2008

The occurrence of ionospheric signatures of plasmaspheric plumes over different longitudinal sectors

E. Yizengaw
University of California, Los Angeles

J. Dewar
Loyola Marymount University

J. MacNeil
Loyola Marymount University

D. Galvan
University of California, Los Angeles

Jeff Sanny
Loyola Marymount University, jeff.sanny@lmu.edu

See next page for additional authors

Authors
E. Yizengaw, J. Dewar, J. MacNeil, D. Galvan, Jeff Sanny, David Berube, and B. Sandel

The occurrence of ionospheric signatures of plasmaspheric plumes over different longitudinal sectors

E. Yizengaw,[1] J. Dewar,[2] J. MacNeil,[2] M. B. Moldwin,[1] D. Galvan,[1] J. Sanny,[2] D. Berube,[1,2] and B. Sandel[3]

Received 5 November 2007; revised 26 March 2008; accepted 5 May 2008; published 27 August 2008.

[1] Plasmaspheric plumes have ionospheric signatures and are observed as storm-enhanced density (SED) in global positioning system (GPS) total electron content (TEC). These ionospheric signatures have been primarily observed over the American sector and in a few limited examples over the European sector. This study examines the longitudinal occurrence frequency of plasmaspheric plumes. We analyzed all images from the Imager for Magnetopause-to-Aurora Global Exploration (IMAGE) Extreme Ultraviolet Imager (EUV) databases for the first half of 2001 and identified a total of 31 distinct plume intervals observed during different storm events. Out of the total IMAGE EUV plumes that we identified, 12 were projected over North America, 10 over Asia, and the remaining 9 were over Europe and the Atlantic Ocean. Using ground-based GPS TEC from MIT's Madrigal database, we searched for corresponding SED/TEC plumes at different longitudinal sector and found 12 ionospheric SED plume signatures over North America, 4 over Europe, and 2 over Asia. This indicates that the observation probability of an ionospheric SED plume when a plasmaspheric plume is seen is 100% in the American sector, 50% in the European sector, and 20% in the Asian sector. This could be due to the fact that the plumes may be either positioned beyond the limit of the ground-based GPS field of view, which happens mainly when there is less plasmaspheric erosion, or are too weak to be detected by the sparse number of GPS receivers over Asia. The in situ plasma densities from the available coincident defense metrological satellite program (DMSP) satellites were also used to study the characteristics of SED/TEC plume at DMSP orbiting altitude (i.e., ~870 km). The TOPographic EXplorer (TOPEX) altimeter TEC also is used to identify the conjugate SED/plume signature over the Southern Hemisphere.

Citation: Yizengaw, E., J. Dewar, J. MacNeil, M. B. Moldwin, D. Galvan, J. Sanny, D. Berube, and B. Sandel (2008), The occurrence of ionospheric signatures of plasmaspheric plumes over different longitudinal sectors, *J. Geophys. Res.*, *113*, A08318, doi:10.1029/2007JA012925.

1. Introduction

[2] The ionosphere has a particularly dramatic effect on radio frequency (RF) systems, especially during geomagnetic storms. During the most disturbed conditions, storms have global impact on the distribution and levels of ionization and the dynamics of the plasmasphere, leading to the formation of plasmaspheric plumes [e.g., *Goldstein and Sandel*, 2005; *Moldwin et al.*, 2004] and their ionospheric signatures observed from the ground [e.g., *Foster et al.*, 2002, 2005a; *Yizengaw et al.*, 2006].

[1]Department of Earth and Space Sciences, Institute of Geophysics and Planetary Physics, University of California, Los Angeles, California, USA.
[2]Frank R. Seaver College of Science and Engineering, Loyola Marymount University, Los Angeles, California, USA.
[3]Lunar and Planetary Laboratory, University of Arizona, Tucson, Arizona, USA.

0148-0227/08/2007JA012925

[3] Flow of energy between the magnetosphere and ionosphere is known to be the dominant source of ionospheric density enhancement at auroral and sub-auroral latitudes. This effect expands to lower latitudes particularly during geomagnetic storms [*Moldwin et al.*, 2004]. The solar-produced F-region ionospheric plasma is transported sunward and poleward from a source region at middle and low latitudes in the afternoon sector, which is associated with the large-scale enhancement of the ionospheric convection electric field during disturbed geomagnetic conditions. This convection forms a latitudinally narrow region of storm-enhanced plasma density (SED) and increased total electron content (TEC), convected sunward extending toward higher latitudes [*Foster*, 1993]. Recent studies [e.g., *Foster et al.*, 2002, 2005a; *Yizengaw et al.*, 2006] show that SED/TEC plumes are associated with the erosion of the outer plasmasphere by strong sub-auroral polarization stream (SAPS) electric fields, and are mapped closely onto the plasmapause and plasmaspheric drainage plumes.

[4] There has been much recent interest in the comparison of plasmaspheric features observed by Imager for Magnetopause-to-Aurora Global Exploration (IMAGE) Extreme Ultraviolet Imager (EUV) [*Burch*, 2000; *Sandel*, 2000], with ionospheric observations. From global positioning system (GPS) maps of TEC, Millstone Hill radar data of SED, and IMAGE EUV images, *Foster et al.* [2002] demonstrated that SED/TEC plumes in the ionosphere mapped directly to plasmaspheric plumes depicted in the IMAGE EUV images during a geomagnetic storm. In the dusk sector where SED/TEC plumes are formed most often, the westward (sunward) convecting SED/TEC plumes are associated with the stripping away of the outer layers of the plasmasphere/ionosphere by the disturbance SAPS electric field [e.g., *Foster et al.*, 2005a and the references therein]. The SAPS electric field is a large poleward directed electric field that is set up to drive a closure current between Region 1 and Region 2 field-aligned current sheets across the low-conductance region, which is equatorward of the auroral electron precipitation region. The magnetospheric origin SAPS electric field increases the recombination rate in the ionospheric F-region by increasing the ion-neutral frictional heating and thus the ion temperature [*Schunk et al.*, 1976; *Pintér et al.*, 2006], resulting in a sharp density gradient at the equatorward edge of the mid-latitude trough region [see *Foster el al.*, 2007; *Yizengaw et al.*, 2005; *Yizengaw and Moldwin*, 2005].

[5] The ionospheric signatures of plasmaspheric plumes have been detected only over North America [e.g., *Foster et al.*, 2002, 2007] and its conjugate over South America [*Coster et al.*, 2003] until *Yizengaw et al.* [2006] reported an observation over the European continent. By combining ground-based GPS TEC, EISCAT (European Incoherent Scatter) radar data, and the DMSP F15 satellite ion drift measurements, *Yizengaw et al.* [2006] found strong enhancements in the electron density over Europe during the recovery phase of a geomagnetic storm on 12 September 2005. This suggested that ionospheric signatures of plasmaspheric plumes may be observed at any longitude provided that there are sufficiently dense arrays of instruments available for their detection.

[6] This premise provides the motivation for our work. The aim of this paper is to present a statistical study of the probability of occurrence of ionospheric SED plume signatures when the plasmaspheric plume is seen at different longitudinal sectors. This study categorized the plasmaspheric plume, using IMAGE EUV observations, by different longitudinal sectors, namely North America, Europe, and Asia. Using the technique described in *Sandel et al.* [2001] and *Foster et al.* [2002], these plumes were then mapped to the simultaneous measurements of ground-based GPS TEC maps from Madrigal TEC database [*Rideout and Coster*, 2006].

[7] In order to identify the conjugate ionospheric signature of SED/TEC plume over the Southern Hemisphere, TOPEX altimeter TEC in the vicinity of the corresponding longitudinal sector and in approximately the same local time sector have also been analyzed. In some longitudinal sectors TOPEX TEC clearly revealed the corresponding sharp boundary between highly enhanced TEC and the greatly reduced value of TEC in the ionospheric trough at the conjugate Southern Hemisphere. DMSP's retarding potential analyzer (RPA) in situ plasma density data are also used to study the characteristics of SED/TEC plumes at DMSP orbiting altitude (i.e., ~870 km).

2. Observations

2.1. IMAGE EUV Plume Observation

[8] For nearly six years between 2000 and 2005, the Imager for Magnetopause-to-Aurora Global Exploration (IMAGE) satellite collected data on the global structure and plasma behavior in the inner magnetosphere. Its array of six instruments provided IMAGE with the capability for imaging neutral atom composition and flux, ultraviolet irradiance, and plasma density gradients [*Burch*, 2003]. Among these instruments was the Extreme Ultraviolet Imager (EUV), which observed EUV at a wavelength of 30.4 nm, resonantly scattered by He^+ in the Earth's plasmasphere. EUV produced global images of the plasmasphere that showed features such as plumes, shoulders, and channels [*Sandel et al.*, 2003]. One of the advantages of such observations is to precisely estimate the global position of the plasmapause. We extracted plasmapause locations manually from several EUV snapshots taken in 2001 by using the IMAGE EUV instrument team developed EUV_IMTOOL program. The location of the plasmapause was determined with an average azimuthal spacing of about an hour of magnetic local time (MLT) [*Goldstein et al.*, 2004]. A typical example of an EUV snapshot image taken on 20 March 2001 at 1443 universal time (UT) is shown in the Figure 1, top, and the corresponding manually extracted plasmapause location is shown in the bottom.

[9] We analyzed all images from the IMAGE EUV database for the first half of 2001, a time when the satellite was at apogee near the North Pole, giving clear pictures of the plasmapause. We identified a total of 136 plumes. However, most of these are the same plumes at different times, and out of the 136 plumes we identified 31 distinct plume intervals (plumes that did not appear more than once at different longitudes in our analyses) observed during different storm events. The plasmapause positions are then projected onto the ionosphere using a dipole magnetic field mapping and overplotted on a 2-D map of a GPS TEC snapshot. This allows us to examine if the SED/TEC plumes, observed from the ground, are associated with the plasmaspheric drainage plume. A list of each plume and the corresponding geomagnetic conditions are given in Table 1. The maximum TEC values and the TEC differences (the difference between the TEC value in the SED/TEC plume and in the vicinity of the trough region) of the SED/TEC plumes (fourth column) are also included in the table.

2.2. SED/TEC Plume Observation Over North America

[10] The simultaneously observed GPS TEC, TOPEX altimeter TEC, DMSP in situ plasma density, and IMAGE EUV image clearly shows the characteristics of the ionospheric signature of the plasmaspheric plume over the North American longitudinal sector as shown in the typical example in Figure 2. A twenty minute average (between

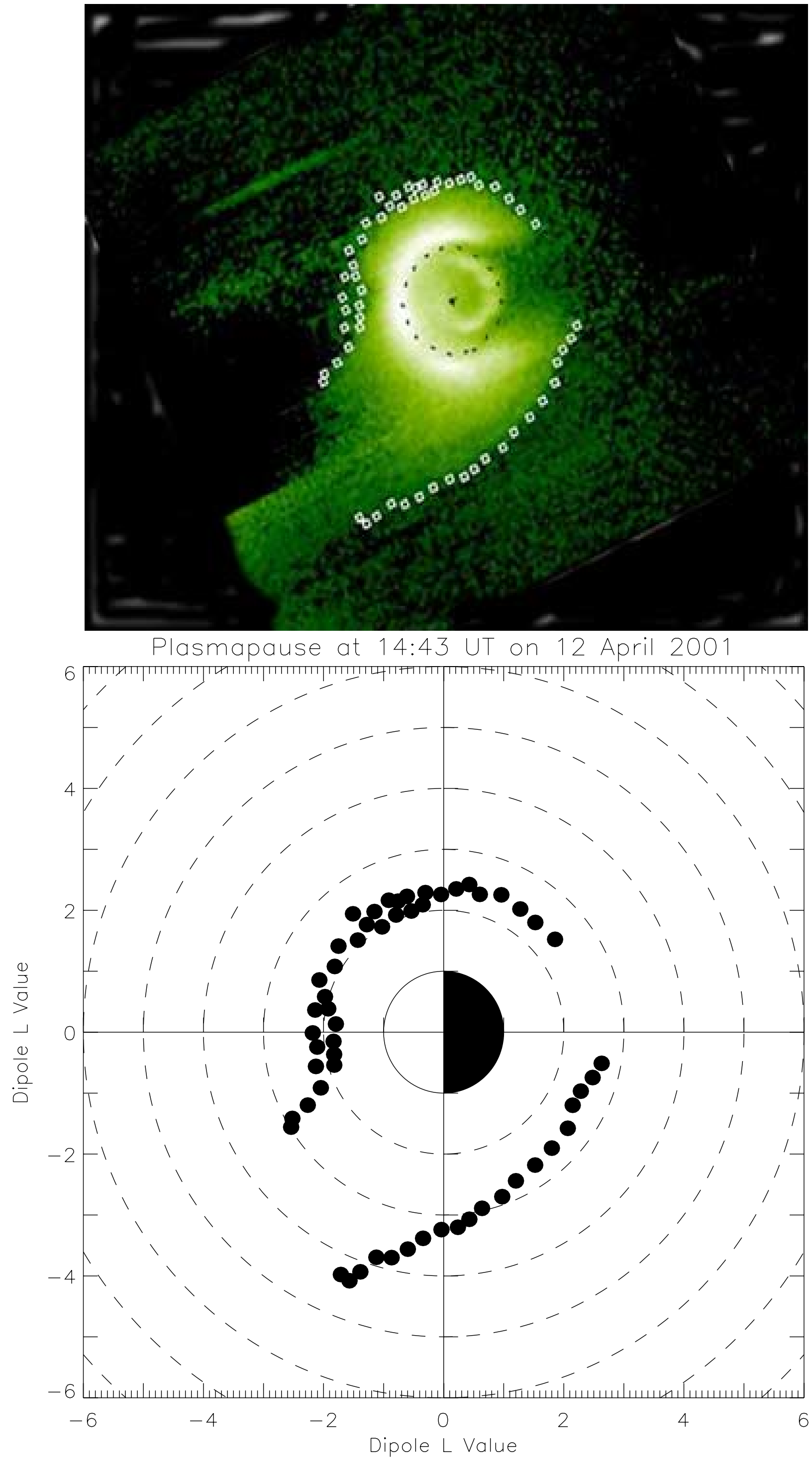

Figure 1. (top) Example of plasmaspheric drainage plume, which is mapped to the magnetic equator (Earth at the center and Sun to the left), as seen by IMAGE EUV at the time and date given below the example, and (bottom panel) solid black circles are manually extracted points along the plasmapause from the EUV snapshot in the top.

0240–0300 UT) snapshot of GPS TEC on 14 February 2001 is shown at the right of the figure. The vertical TECs have been binned in 2° × 3° latitude/longitude bins and no interpolation has been used to produce each GPS TEC map. The dashed black curve depicts the geomagnetic equator. A sharp boundary between the enhanced TEC, which is referred as SED/TEC plume, and the greatly reduced value of TEC is clearly shown across the United State in the right of Figure 2. This SED/TEC plume of ionization located at the equatorward edge of the main ionospheric trough is

Table 1. Characteristics of All 31 Plumes Observed in This Statistical Study[a]

Date/Time	Geomagnetic Condition (Kp)	Plume Locations	Maximum TEC (TEC Difference)	EUV Plumes			SED/TEC plumes		
				NA	EU	AS	NA	EU	AS
024/2331	5	N.A. east coast	>30 (>20)	1			1		
031/2333	4	N.A. east coast	>45 (>35)	1			1		
044/1454	4	Europe	>30 (>20)		1			1	
045/0259	5	N.A. West Coast	>35 (>25)	1			1		
054/1736	3	Europe	>35 (>25)		1			1	
055/0541	2	East Asia	lack of TEC			1			–
064/0404	5	N.A. West Coast	>30 (>22)	1			1		
065/0819	2	Asia	>27 (>15)			1			1
072/1045	3	East Asia	lack of TEC			1			–
078/1037	2	East Asia	lack of TEC			1			–
079/0043	7	N.A. West Coast	>45 (>30)	1			1		
079/1450	7	Europe/Atlantic	>30 (>20)		1			1	
082/1425	5	Europe/Atlantic	>25 (>15)		1			1	
087/0556	6	N.A. West Coast	>45 (>32)	1			1		
088/1040	6	Asia	lack of TEC			1			–
090/2109	9	N.A.	>45 (>30)	1			1		
092/0152	5	N.A. West Coast	>50 (>35)	1			1		
097/0750	4	East Asia	lack of TEC			1			–
099/1930	7	N.A. east coast	>45 (>25)	1			1		
102/0138	8	N.A. West Coast	>40 (>32)	1			1		
108/1349	7	Asia	>20 (>10)			1			1
118/1903	6	Atlantic	lack of TEC		1			–	
129/0700	5	Asia	lack of TEC			1			–
132/1944	5	Atlantic	lack of TEC		1			–	
139/1244	4	Asia	lack of TEC			1			–
148/2106	4	N.A. east coast	>38 (>23)	1			1		
153/1632	5	Europe	no TEC gradient		1			–	
161/0734	6	Russia/Alaska	lack of TEC			1			–
169/1540	5	Atlantic	no TEC gradient		1			–	
172/1532	4	Europe	lack of TEC		1			–	
177/2357	4	N.A. West Coast	>35 (>20)	1			1		
Total number of plumes at different sectors				12	9	10	12	4	2

[a]Plumes extracted from IMAGE EUV data and SED/TEC plumes and their corresponding locations over the North American (NA), European (EU), and Asian (AS) longitudinal sectors are identified. The corresponding geomagnetic conditions (second column) and the maximum TEC values and TEC differences of the plumes (fourth column) are included, and the numbers in bracket refer to the TEC difference.

streaming westward [see *Foster et al.*, 2004 for detail]. Similar plume signatures have been previously reported [e.g., *Foster et al.*, 2002, 2005a, 2007].

[11] The simultaneously determined position of the plasmapause estimated from the corresponding IMAGE EUV image is overplotted (open triangles connected by red dash-dot curves) on the global GPS TEC map. During the 14 February storm period at 0259 UT IMAGE EUV observed an eroded plasmasphere with a plasmapause close to L = 2.8 or less between 1200 and 1500 MLT (~140°E and 180°E) and the formation of a plasmaspheric plume co-located with the projected position of the SED/TEC plume. The in situ density observation from DMSP satellite data has been also used to confirm the ground-based GPS plume observation. The in situ plasma density from the coincident passes of two DMSP satellites (F13 and F15) is shown in the left of Figure 2. The ionospheric tracks of the DMSP satellites are shown in the right, with the red curve for F13 and black for F15. As can be seen in the left, sharp density depletions (indicated by blue horizontal arrow) are observed when F13 satellite cross the SED/TEC plume boundary poleward into the trough region. Very sharp density enhancements were observed by both DMSP satellites when they cross northward of the SED/TEC plume detected by the available ground-based GPS receivers as indicated by the upward blue arrow. In the Southern Hemisphere, there is an indication of conjugate plume. A localized TEC enhancement is observed at high-latitudes between 120°E and 150°E longitude, and it is a clear indication that this localized TEC enhancement could be in the region of the south-west plume expansion region which is indicated by faint blue dashed line. This faint blue lines (both in the southern and northern hemisphere) were extended manually in order to accommodate and follow the trajectory of the enhanced density observed by different instruments. The SED/TEC plume transported from subauroral latitudes (over south of Alaska as shown in Figure 2) along the sunward convection pattern through the dayside cusp region between 180°E–200°E (1500–1600 LT). As can be seen between 250°E–300°E (2000–2300 LT) in the right of Figure 2, the plume then transported into polar cap, exiting the polar region in the nightside of northern Canada. The dispersed enhanced TEC signature over northern Canada, therefore, could be the continuous streaming of enhanced density, forming the polar tongue of ionization (TOI) which is consistent with [*Foster et al.*, 2005a] multi instrument observations. The DMSP F13 (red curve) and F15 (black curve) crossed the projected path of TOI, which is marked by faint blue solid curves in the northern hemisphere (see Figure 2), approximately the same local time as the GPS TEC observation. Interestingly, the spacecraft detected enhanced density

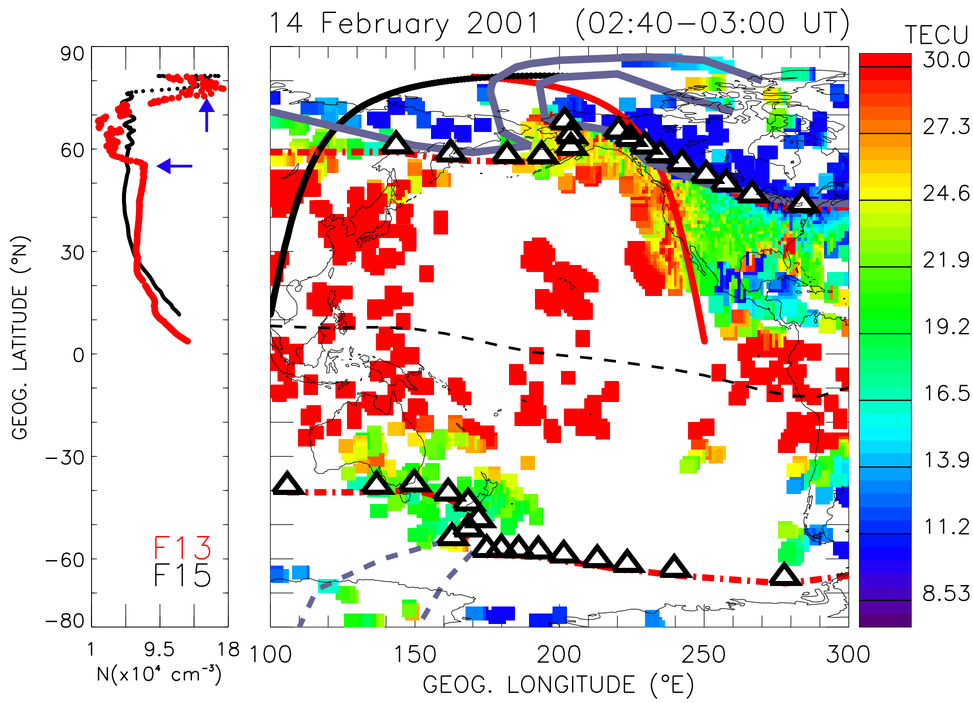

Figure 2. (Left) The in situ plasma density at the DMSP orbiting altitude; red and black curves represent DMSP F13 and F15, respectively. (Right) The 20-minute average 2-D map of a GPS TEC snapshot of SED/TEC plume on 14 February 2001 at 0240–0300 UT over the North American sector, IMAGE EUV plasmapause positions (open triangles), and the ground tracks of DMSP F13 (red curve) and F15 (black curve). The faint blue solid curve at the north and dashed curves at the Southern Hemisphere depict a projected extension of the SED/TEC plume.

(from $\sim 7 \times 10^4$ cm^{-3} outside to $\sim 1.8 \times 10^5$ cm^{-3} inside the path) inside the projected path of TOI as shown in Figure 2, left, which is indicated by upward arrow. *Foster et al.* [2005a] described in detail about the source and transport of TOI across the polar cap region. Unfortunately, there are no GPS receivers in the region where DMPS detected these enhancements for confirmation.

3. SED/TEC Plume Observation Over Europe

[12] A pronounced band of storm-enhanced density extending from south of Europe across northern England and into the Atlantic Ocean has been observed during a different magnetic storm period in 2001. The SED/TEC plume is presented in Figure 3. The figure is in the identical format as Figure 2, but Figure 3 presents the SED/TEC plume observation over Europe on 20 March 2001 at 1440–1500 UT. Similarly, Figure 3 also clearly reveals a sharp boundary between SED/TEC plume and the depleted TEC, which is shown across the middle of Europe and extended across Greenland. TOPEX TEC also detected this sharp boundary at the conjugate (southern) hemisphere as shown in the left of Figure 3. TOPEX altimeter data are found to be very important in order to detect SED/TEC plumes in the region where there are no GPS receivers available, most importantly to detect conjugate plume over the ocean in the Southern Hemisphere. The TOPEX altimeter TEC (blue curve in the left) dropped from ~50 TECU to 8 TECU right at the plasmapause signature. The position of this sharp TEC gradient (sharp boundary between plume and depleted TEC) and the plasmapause are also coincident as shown in the right, especially in the Southern Hemisphere. Open triangles in the right of the figure depict the position of the plasmapause estimated from the corresponding IMAGE EUV observation. The conjugate SED/TEC plume signature, which is aligned with the plasmapause locations (open triangles), is also evident in the Southern Hemisphere as shown in Figure 3 between 20°W and 5°E longitudes. The maximum TEC value in this conjugate plume is about 40 TECU or more providing a TEC difference of about 24 TECU between plume and trough. The closely aligned location of the plasmapause and the sharp SED/TEC gradient indicates good co-location of plasmaspheric plume and the projected position of the SED/TEC plume. Similarly, the in situ plasma density from the coincident pass of DMSP satellite (F15) is shown in the left of Figure 3. DMSP F15 (black curve) crosses the SED/TEC plume and verifies the existence of the stretched SED/TEC plumes over the Atlantic Ocean all the way through the Labrador Sea by showing the in situ density enhancement centered at ~65°N geographic (indicated by upward red arrow in the left of Figure 3). A sharp density difference (from $\sim 8.5 \times 10^4$ cm^{-3} outside to $\sim 2.7 \times 10^5$ cm^{-3} inside the plume) is also evident when DMSP F15 entered into the trough region on both sides (equatorward and poleward) of the stretched SED/TEC plume.

4. SED/TEC Plume Observation Over Asia

[13] Although there are many ground-based GPS receivers available over the Russian/Asian sector, there is

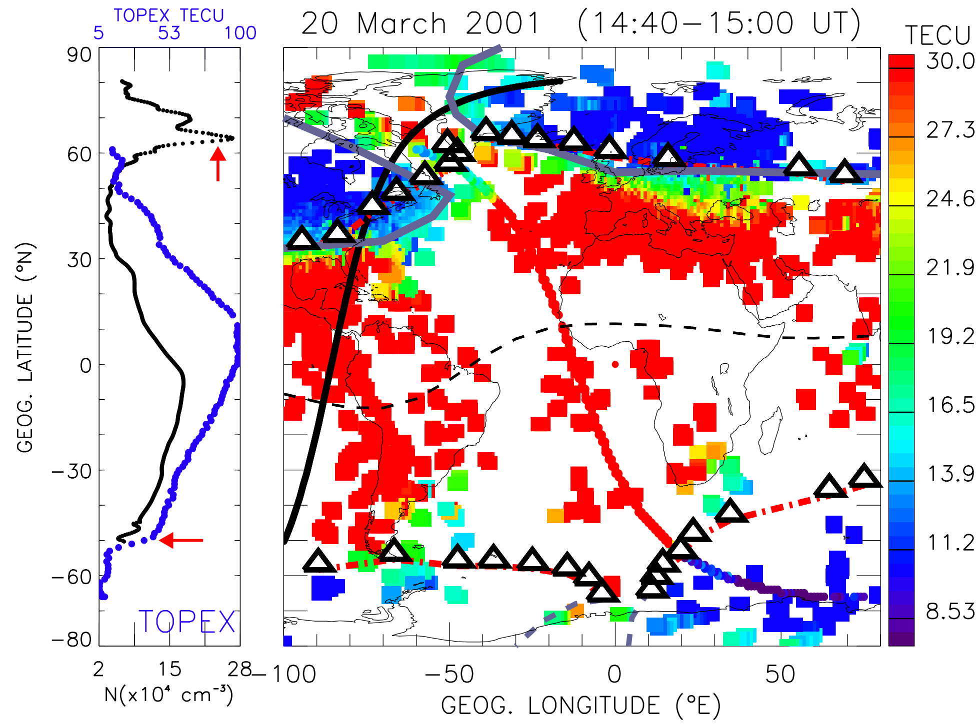

Figure 3. Same as Figure 2 but for snapshot of SED/TEC plume taken on 20 March 2001 at 1440–1500 UT over the European longitudinal sector. It also includes TOPEX altimeter TEC in the left (blue curve) and its ground track is overplotted in the right. DMSP F15 in situ plasma density is also shown in the left (black curve). Note the separate TOPEX TEC scale shown at the top of the left.

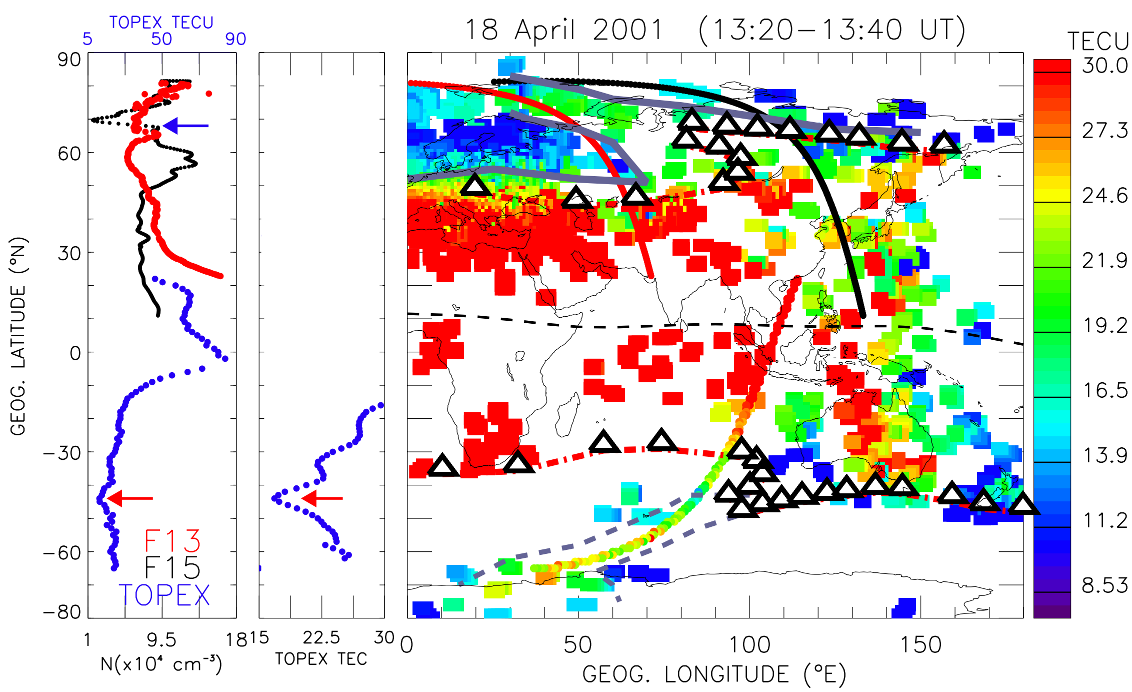

Figure 4. Same as Figure 3 but for snapshot of SED/TEC plume taken on 18 April 2001 at 1320–1340 UT over the Asian longitudinal sector. The middle shows the TOPEX TEC depletion seen at ∼45°S latitude with an enhanced scale.

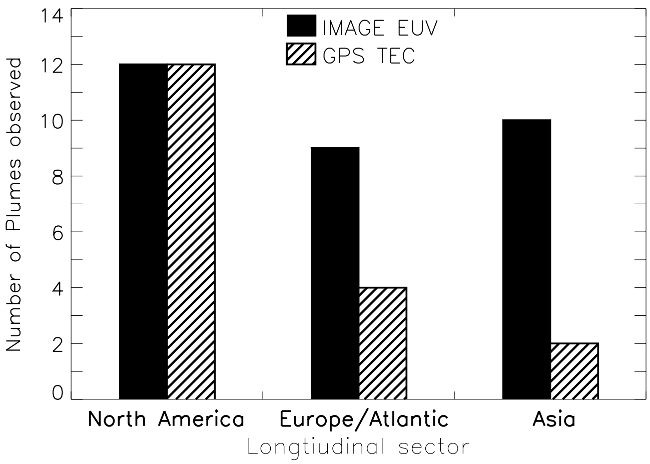

Figure 5. The histogram of plume observations from the ground (SED/TEC plume) and from space (IMAGE EUV) at various longitudinal sectors.

not the same density of receivers as over North America and Europe. The projection of a plasmaspheric plume (estimated from IMAGE EUV image) observed over Asia is shown in Figure 4. Figure 4 has the same format as Figure 2, but Figure 4 is for 18 April 2001 at 1320 – 1340 UT. However, the SED/TEC plume is very weak compared to the SED/TEC plume observed over North American and Europe. Our twenty minute average TEC map detected a corresponding weakly enhanced TEC band extending from East Asia across northern Russia and into the northern Scandinavia as marked by faint blue solid line in Figure 4. The projected IMAGE EUV estimated plasmapause positions (open triangles) appears to be inside the faint blue solid curves, indicating the clear collocation of SED/TEC plume and plasmaspheric plume in the Asian sector. This could be taken as the first distinct SED/TEC plume observed over Asia. *Maruyama* [2006] presented ionospheric signature of plumes over Japan using ground-based GPS TEC, but he did not confirm it with other independent observations such as IMAGE EUV.

[14] Similarly, in this longitudinal sector there is an indication of conjugate plume in the Southern Hemisphere. The projected extension of plume, which is bordered by the plasmapause positions [e.g., *Foster et al.*, 2002], is drawn (faint blue dashed curves) and inside this region a localized TEC enhancement is observed. The TOPEX altimeter TECs that are taken within the corresponding time interval observe TEC enhancement in this region too. TOPEX also detect a sharp TEC depletion center at 45°S as shown in the left (blue curve) and more clearly in the middle of the figure with more than 6 TECU difference between trough minimum and equator or poleward side of the trough as indicated by red arrow. This depletion coincides with the plasmapause position at the extended plume as shown in the right of the figure marked by dashed faint blue line.

[15] DMSP F15 (black curve) flew over this region and detected a very sharp density depletion, centered at ~70°N (indicated by the blue arrow in the left of Figure 4). DMSP F13 (red curve) that flew across the sharp density gradient region also shows in situ density depletion, centered at ~60°N in the left of the figure, at an altitude of DMSP orbiting altitude (~870 km). Both DMSP spacecraft flew across the extended SED/TEC plume and confirmed the ground-based GPS SED/TEC plume observation by detecting density enhancement in the region. The density enhancement for both spacecraft was from $\sim 6.5 \times 10^4$ cm^{-3} at about 72°N (outside the SED/TEC plume) to $\sim 9.0 \times 10^4$ cm^{-3} at about 80°N (inside the SED/TEC plume).

5. Discussion

[16] The sharp TEC and in-situ density depletion shown in the given examples (Figures 2–4) indicate the TEC (in-situ density) difference between enhanced (SED/TEC plume) and depleted region that is driven away by SAPS electric field. The SAPS electric field is responsible for the plasmasphere boundary layer (plasmapause) and the formation of SED/TEC plume. The equatorward edge of this depleted density also coincides with the position of plasmapause position extracted from IMAGE EUV (white triangle).

[17] Our study addresses the categorization of IMAGE EUV plume by different longitudinal sectors. The corresponding ionospheric signatures of the plasmaspheric plume observations are observed at different longitudinal sectors. Previously, the ionospheric plasmaspheric plume signatures were often observed over the North American sector. Recently, *Yizengaw et al.* [2006] published the first plume observation over Europe and suggested that the plumes' signature can be observed at any longitudinal sector as long as there are ground-based instruments in the region to detect them. This premise provided the motivation to perform a systematic SED/TEC plume search at different longitudinal sectors. Out of the total IMAGE EUV plumes that we identified, 12 were projected over North American, 10 over Asia, and the remaining 9 were over Europe and the Atlantic Ocean as shown in Table 1 and in the histogram plot shown in Figure 5. The simultaneously measured ground-based GPS TEC also detected ionospheric SED/TEC plumes over the corresponding longitudinal sectors as indicated by the line solid bars in Figure 5. The figure presents histograms of the number of plumes observed both from the ground (ground-based GPS TEC maps) and from space (IMAGE EUV images) as a function of longitudinal sector. As can be seen in the figure, twelve SED/TEC plumes are detected over North America, four over Europe, and only two over Asia. This indicates that the probability of observation of an ionospheric SED plume when a plasmaspheric plume is seen is 100% in the American sector, 50% in the European sector, and 20% in the Asian sector. The maximum observation probability over North America has been suggested because of the geomagnetic dip equator. Because of the dipole tilt toward North America, low geographic latitudes are at mid-to-high geomagnetic latitudes in the northern hemisphere and high geographic latitudes are at low geomagnetic latitudes in the south. The maximum TEC values of the SED/TEC plumes (see the fourth column in Table 1) over North American sector are larger than plumes over the European and Asian sectors, making the North American SED/TEC plume more easily identifiable compared to the European and Asian sectors. This could be due to the existence of strong equatorial

anomaly in the American sector [see *Foster and Coster*, 2007 and the reference therein]. However, the lower SED/TEC plume occurrence probability over Asia could be due to at least two reasons. The first is that the SED/TEC plume is very weak and difficult to detect by the sparse number of GPS receivers in the region. The second reason is that since the magnetic equator is shifted to the north, the high geographic latitudes will appear to be at low geomagnetic latitudes. This places the projected plume and thus SED/TEC plume at relatively high geographic latitudes making it difficult to detect SED/TEC plumes in this sector as it may occur outside most GPS receivers' field of view.

[18] Using the combination of simultaneous measurements of ground-based GPS TEC and space-based IMAGE EUV observations, we demonstrate that the IMAGE EUV plumes can be found in any longitudinal sectors. The qualitative comparison of SED/TEC plumes and plumes observed by IMAGE EUV for different L-shell values of the plasmapause have been performed, and good agreement was found when the plasmapause was located at lower L-shell values ($L < 2.6$). This clearly indicates that as the plasmapause is eroded to lower L-shells, the SED/TEC plume is observed in the mid latitude region where we have dense ground-based GPS receiver coverage. However, when the plasmapause is at higher L-shell, the SED/TEC plume is located at higher latitudes where few GPS receivers are available. This creates poor agreement between the simultaneously observed SED/TEC plumes and IMAGE EUV's plume, especially over the European and Asian sectors. For example, a plasmapause at $L = 3.0$ has an ionospheric foot print at a geographic latitude of above 61° over the Russian/Asian sector and ~57° over Europe. However, the same plasmapause has an ionospheric foot print at about 42° geographic over the North American sector. Therefore, in order to detect the associated SED/TEC plume over the European and the Russian/Asian sectors; the plasmasphere must be eroded to lower L-shell values. Therefore, because of the reasons mentioned above, a pronounced difference in plume observations from the ground and from space is evident over Europe and Asian sectors as shown in Figure 5. In this region ground-based GPS TEC only detected four (two) SED/TEC plumes out of the corresponding nine (ten) plasmaspheric drainage plumes observed by IMAGE EUV over Europe (Asia). This could be due to the fact that the plumes may be either positioned beyond the limit of the ground-based GPS field of view, which happens mainly when there is less plasmaspheric erosion, or are too weak to be detected by the sparse number of GPS receivers.

6. Conclusion

[19] For the first time a survey using multi-instrument observations clearly determines the correspondence of IMAGE EUV plasmaspheric plumes and their SED/TEC plume counterparts in different longitudinal sectors. Although the number of ground-based GPS receivers are limited in longitude sectors other than North America and Europe, the space-based (IMAGE EUV) observation data show that plumes can form over any part of the globe. However, SED/TEC plume features were previously observed over North American sector. It was suggested that the equatorward offset of the geomagnetic pole at those longitudes could probably play a major role for the SED/TEC plume formation in this region [*Foster et al.*, 2005b].

[20] Out of a total of 31 distinct plasmaspheric plumes that we analyzed for this survey, twelve were projected over North America, nine over Europe, and ten over Asia. We also detected the corresponding ionospheric SED/TEC plume signatures and found twelve SED/TEC plume over North America, four over Europe, and two over Asia. This clearly indicates that the probability of observation of an ionospheric SED/TEC plume when a plasmaspheric plume is seen is 100% in the American sector, 50% in the European sector, and 20% in the Asian sector. The magnetic equator shift to the south in the American longitudes is considered as a prime reason for the maximum occurrence probability of SED/TEC plume over North American. In the European and especially the Asian sectors the magnetic equator shifts to the north, placing this region at high geographic latitudes so that the SED/TEC plumes typically extend beyond the field of view of the available GPS receiver networks. This could be one reason for less observation probability of SED/TEC plume over these regions. However, this doesn't mean that the SED/TEC plume is not there when IMAGE EUV observes a plasmaspheric plume in the region, but it may be very weak to be detected by sparse number of GPS receivers in the region, especially over Asian sector. From our survey we found out that the SED/TEC plume over Europe and Asia, especially over Asia, are weaker than the ones observed over North America as can be seen in Figures 2–4. The ionospheric SED/TEC plume shown in Figure 4 is the first distinct plume observed over Asian sector. *Maruyama* [2006] presented ionospheric signature of plumes over Japan using ground-based GPS TEC. However, it was not confirmed with other independent measurements such as IMAGE EUV. However, the SED/TEC plume detected on 18 April 2001 at 1320–1340 UT shows a clear and good coincidence with plasmaspheric plume observed from space using IMAGE EUV. The two DMSP spacecraft (F13 and F15) also confirm the SED/TEC plume observation by detecting a significant density enhancement in the vicinity of the plume at their orbiting altitude (~870 km). A similar SED/TEC plume over Asia is also observed (not shown here) on 06 March 2001 at 0800–0820 UT. This study clearly demonstrates that the plasmaspheric drainage plumes can be observed at any longitudinal sector, potentially contributing to the degradation of our communication and navigation systems around the globe.

[21] **Acknowledgments.** The authors are grateful to MIT Haystack Observatory for GPS TEC data obtained from their Madrigal data center. This research work was supported by NSF grants ATM-0524711 and ATM-0348398 and by NASA IHY grant NNX07AM22G. Works at the University of Arizona and Loyola Marymount University were supported by a subcontract under NASA contract NAS5-96020 to Southwest Research Institute and by NSF grant ATM-0350502, respectively.

[22] Zuyin Pu thanks John Foster and another reviewer for their assistance in evaluating manuscript this paper.

References

Burch, J. L. (2000), IMAGE mission overview, *Space Sci. Rev.*, *91*, 1–14.

Coster, A., P. Erickson, and J. C. Foster (2003), Monitoring the ionosphere with GPS, *GPS*, 40–45.

Foster, J. C. (1993), Storm time plasma transport at middle and high latitudes, *J. Geophys. Res.*, *98*(A2), 1675–1689.

Foster, J. C., and A. J. Coster (2007), Conjugate localized enhancement of total electron content at low latitudes in the American sector, *J. Atmos. Space Terr. Phys.*, *69*, 1241–1252.
Foster, J. C., P. J. Erickson, A. J. Coster, J. Goldstein, and F. J. Rich (2002), Ionospheric signatures of plasmaspheric tails, *Geophys. Res. Lett.*, *29*(13), 1623, doi:10.1029/2002GL015067.
Foster, J. C., A. J. Coster, P. J. Erickson, F. J. Rich, and B. R. Sandel (2004), Stormtime observations of the flux of plasmaspheric ions to the dayside cusp/magnetopause, *Geophys. Res. Lett.*, *31*, L08809, doi:10.1029/2004GL020082.
Foster, J. C., et al. (2005a), Multiradar observations of the polar tongue of ionization, *J. Geophys. Res.*, *110*, A09S31, doi:10.1029/2004JA010928.
Foster, J. C., A. J. Coster, P. J. Erickson, W. Rideout, F. J. Rich, T. J. Immel, and B. R. Sandel (2005b), Redistribution of the stormtime ionosphere and the formation of the plasmaspheric bulge, in *Inner Magnetosphere Interactions: New Perspectives From Imaging*, edited by J. Burch and M. Schultz, pp. 277–289, AGU Press, Washington, D. C.
Foster, J. C., W. Rideout, B. Sandel, W. T. Forrester, and F. J. Rich (2007), On the relationship of SAPS to storm enhanced density, *J. Atmos. Space Terr. Phys.*, *69*, 303–313.
Goldstein, J., and B. R. Sandel (2005), The global pattern of evolution of plasmaspheric drainage plumes, *Inner Magnetosphere Interactions: New Perspectives From Imaging*, *Geophysical. Monograph Series*, *159*, p. 1.
Goldstein, J., B. R. Sandel, M. F. Thomsen, M. Spasojeviæ, and P. H. Reiff (2004), Simultaneous remote sensing and in situ observations of plasmaspheric drainage plumes, *J. Geophys. Res.*, *109*, A03202, doi:10.1029/2003JA010281.
Maruyama, T. (2006), Extreme enhancement in total electron content after sunset on 8 November 2004 and its connection with storm enhanced density, *Geophys. Res. Lett.*, *33*, L20111, doi:10.1029/2006GL027367.
Moldwin, M. B., J. Howard, J. Sanny, J. D. Bocchicchio, H. K. Rassoul, and R. R. Anderson (2004), Plasmaspheric plumes: CRRES observations of enhanced density beyond the plasmapause, *J. Geophys. Res.*, *109*, A05202, doi:10.1029/2003JA010320.
Pintér, B., S. D. Thom, R. Balthazor, H. Vo, and G. J. Bailey (2006), Modeling subauroral polarization streams equatorward of the plasmapause footprints, *J. Geophys. Res.*, *111*, A10306, doi:10.1029/2005JA011457.
Rideout, W., and A. Coster (2006), Automated GPS processing for global total electron content data, *GPS Solution*, doi:10.1007/s10291-006-0029-5.
Sandel, B. R., et al. (2000), The Extreme Ultraviolet Imager investigation for the IMAGE mission, *Space Sci. Rev.*, *91*(1/2), 197–242.
Sandel, B. R., R. A. King, W. T. Forrester, D. L. Gallagher, A. L. Broadfoot, and C. C. Curtis (2001), Initial results from the IMAGE Extreme Ultraviolet Imager, *Geophys. Res. Lett.*, *28*(8), 1439–1442.
Sandel, B. R., J. Goldstein, D. L. Gallagher, and M. Spasojevic (2003), Extreme Ultraviolet Imager observations of the structure and dynamics of the plasmasphere, *Space Sci. Rev.*, *109*(1), 25–46.
Schunk, R. W., P. M. Banks, and W. J. Raitt (1976), Effects of electric fields and other processes upon the nighttime high-latitude F layer, *J. Geophys. Res.*, *81*, 3271–3282.
Yizengaw, E., and M. B. Moldwin (2005), The altitude extension of the mid-latitude trough and its correlation with plasmapause position, *Geophys. Res. Lett.*, *32*, L09105, doi:10.1029/2005GL022854.
Yizengaw, E., H. Wei, B. Moldwin, D. Galvan, L. Mandrake, A. Mannucci, and X. Pi (2005), The correlation between mid-latitude trough and the plasmapause, *Geophys. Res. Lett.*, *32*, L10102, doi:10.1029/2005GL022954.
Yizengaw, E., M. B. Moldwin, and D. A. Galvan (2006), Ionospheric signatures of a plasmaspheric plume over Europe, *Geophys. Res. Lett.*, *33*, L17103, doi:10.1029/2006GL026597.

D. Berube, D. Galvan, M. B. Moldwin, and E. Yizengaw, Department of Earth and Space Sciences, Institute of Geophysics and Planetary Physics, University of California, Los Angeles, CA 90095, USA. (ekassie@igpp.ucla.edu)

J. Dewar, J. MacNeil, and J. Sanny, Frank R. Seaver College of Science and Engineering, Loyola Marymount University, Los Angeles, CA 90045, USA.

B. Sandel, Lunar and Planetary Laboratory, University of Arizona, Tucson, AZ 85721, USA.